RSC Advances

This is an *Accepted Manuscript*, which has been through the Royal Society of Chemistry peer review process and has been accepted for publication.

Accepted Manuscripts are published online shortly after acceptance, before technical editing, formatting and proof reading. Using this free service, authors can make their results available to the community, in citable form, before we publish the edited article. This *Accepted Manuscript* will be replaced by the edited, formatted and paginated article as soon as this is available.

You can find more information about *Accepted Manuscripts* in the **Information for Authors**.

ROYAL SOCIETY OF CHEMISTRY

www.rsc.org/advances

Toughening of epoxy resin using Zn$_4$O (1,4-benzenedicarboxylate)$_3$ metal organic framework

Manju,[a,b] Prasun Kumar Roy,[a*] Arunachalam Ramanan[b**]

[a] Centre for Fire, Explosive and Environment Safety, DRDO, Delhi-54, India

[b] Department of Chemistry, Indian Institute of Technology Delhi, New Delhi-16, India

Corresponding author. Tel.:+911123907191; Fax:+911123819547.

Co-Corresponding author. Tel.:+911126591507; Fax:+911126581102.

* E-mail addresses:pk_roy2000@yahoo.com (Prasun Kumar Roy)

** aramanan@chemistry.iitd.ac.in, aramanan57@gmail.com.(A Ramanan)

Abstract

In this paper, we have demonstrated the potential of the well-known microporous MOF 5 towards toughening of a cycloaliphatic epoxy resin by preparing Epoxy-MOF 5 composites (0.1-0.7% w/w). Introduction of MOF 5 led to significant stiffening and improvement in dynamic properties as indicated by 68% increase in impact strength and 230% increase in fracture energy at an optimal loading of 0.3% w/w. A comparison of the mechanical response under different strain rates established the strain rate sensitivity of the composites, which is of relevance under blast loading conditions. We also performed fractographic analysis of the ruptured surface to understand the underlying mechanism behind the improvement in toughness.

1. Introduction

Physical blending and chemical crosslinking are fundamental techniques used to alter structure-property relationship of polymeric materials. These methodologies have proved to be successful in improving the fracture toughness of thermosets by transforming their "brittle" mechanical response to "ductile" mode. Polyepoxies belong to a sub-class of high-performance thermosetting polymers, which are the most commonly used matrix resin for fibre-reinforced composites. Epoxies are well known for their excellent mechanical properties, particularly high strength and large modulus, low creep and thermal stability. However, their inherently crosslinked structure leads to its brittle failure, especially under impact induced dynamic loadings. Numerous methods have been adopted to realize toughening of epoxies, the most common being inclusion of fillers in the otherwise homogenous polymeric matrix. Although elastomeric, [1-6] thermoplastics, [7-11] nanomaterials [12] and rigid particulates,[13-16] are conventionally used for epoxy toughening, the search for alternate materials has received much attention.

In this context, metal-organic frameworks (MOFs) offer an interesting class of hybrid materials and could be readily obtained through a self assembly process between organic ligands and suitable metal cations.[17-19] High surface areas, large porosities and flexibility to incorporate functionality makes MOFs particularly attractive for a wide range of applications in preference to zeolites and activated carbonaceous substrates. Recently, MOFs are being investigated for its ability to absorb mechanical energy;[20-22] the dimensionality of the metal–organic interaction is susceptible to undergo elastic transformations under specified directions which in turn can affect their physical properties. For example, MIL 47 (vanadium oxide terephthalate) underwent perfectly elastic deformation with loadings upto 340 MPa.[23] In another study, HKUST 1 (copper-benzene 1,3,5-tricarboxylic acid) was found to exhibit anisotropy in structural collapse. MOF 5

3

has been reported to mechanically respond as elastic materials, with a theoretical maximum Young's modulus of the order of 19.7 GPa, and anisotropy of 2.1.[24] A few MOF based composites with thermoplastics have been reported to exhibit significant improvement in mechanical properties; HKUST - poly(lactide) composite showed an increase in fracture toughness (399 %), however the tensile strength was adversely affected. [25-28]

Incorporation of mechanically responsive microporous MOFs within a thermosetting resin can improve mechanical properties of the base polymer. A major impediment in preparing epoxy based composites concerns the dispersion of the filler and in most cases, the filler surface needs to be treated for achieving proper dispersion and load transfer. [29] We believe that MOFs being a hybrid material can take advantage of its organic groups and disperse uniformly in the epoxy matrix. In addition, the high surface area of MOF is expected to result in constructive interfacial interactions between the polymer and the filler surface. [30] This paper is an attempt to illustrate the potential of MOF 5 towards toughening of epoxy, and quantify its energy absorption characteristics under varied mechanical loadings.

2. Experimental

2.1. Materials

Epoxy resin (Ciba Geigy, Araldite CY 230; epoxy equivalent 190 eq/g) and triethyltetraamine hardener (TETA, HY 951; amine content 32 eq kg^{-1}) was used as received. Zinc nitrate trihydrate ('AR' grade, E.Merck), terephthalic acid (TPA) ('AR' grade, E.Merck), N,N- Dimethylformamide ('AR' grade, E. Merck) was used without further purification. HPLC grade water was used throughout the course of this work.

2.2. Supramolecular assembly of metal organic framework

MOF 5 was prepared as per the procedure reported in our previous papers.[31, 32] In brief, separate solution of TPA (5.06 g, 30.5 mmol) and zinc acetate dihydrate (16.99 g, 77.4 mmol) were prepared in DMF, which were mixed and allowed to react for 2.5 h under stirring. The resulting crystallites were filtered, washed repeatedly with DMF and stored under desiccation.

2.3. Preparation of epoxy composites

Epoxy composites containing varying loadings of MOF 5 (0.1- 0.7 %w/w) were prepared by dispersing requisite amounts into the epoxy resin by ultrasonication for 30 min at 33 kHz. TETA hardener was subsequently added to the mixture (13 phr), to achieve an amine: epoxide stoichiometry of 1:1 and the same was ultrasonicated for another 15 minutes to remove entrapped air bubbles. The suspension was degassed under vacuum and transferred to silicone molds, where the curing reaction was allowed to proceed at 30 °C for 24 h. Neat epoxy specimens were also prepared under similar conditions. Details of the amount of MOF 5 and hardener used for the preparation of composites, along with the sample designation are comprehensively listed in the supplementary section (Table S 1). The samples have been designated as EP followed by the concentration of MOF 5 ($\times$10) used for its preparation, i.e. EP5MOF refers to a composition containing 0.5% MOF 5.

2.4. Characterization methods

Powder XRD analyses of the samples were carried out on Bruker D8 advanced diffractometer equipped with nickel filter CuKα radiation. FTIR spectra was recorded in the wavelength range 4000 - 600 cm^{-1} using a Thermo Fisher FTIR analyser (NICOLET 8700) with an attenuated total reflectance (ATR) crystal accessory. The textural property of MOF 5 was determined by N_2 adsorption– desorption on a surface area analyzer (Micromeritics ASAP 2020, Novcross, Georgia) equipment. For this purpose, the sample was initially out gassed under

vacuum (10^{-6} Torr) at 150°C for 16 h and the nitrogen adsorbate was pulsed at 77 K. Surface area was calculated from the linear part of the BET plot. Calorimetric studies were performed on a Differential Scanning Calorimeter (TA instruments Q 20). Thermal degradation behavior was investigated using Perkin Elmer Diamond STG-DTA-DSC under air atmosphere in the temperature range of 50-800 °C at a heating rate of 10 °C/min. The surface morphology of the unsputtered samples was studied using a Scanning Electron Microscope (Zeiss EVO MA15) under an acceleration voltage of 1kV.

Quasi-static mechanical properties were determined as per ASTM method D638 using a Universal Testing System (International equipments) at ambient temperature. The samples were subjected to a cross head speed of 50 mm min^{-1}. The notched izod impact strength of the specimens was determined using an impact strength testing machine (International Equipments, India). Notched flexural testing of the samples was performed under three point single edge notch bending mode. For this purpose, specimens (127 mm length x 12.5 mm width x 3.5 mm thickness and 3 mm notch) were prepared and the samples were subjected to a deformation rate of 2 mm min^{-1} while maintaining a span length of 60 mm. The mode I critical stress intensity factor (K_{IC}) of the samples was determined as per the following equation: [33]

$$K_{Ic} = \frac{3 \times P \times L \times a^{1/2}}{2 \times B \times w^2} Y(\frac{a}{w}) \ldots\ldots\ldots\ldots(1)$$

Where, P, L and B refer to the load at break, span length and sample thickness respectively. The geometry factor, $Y(\frac{a}{w})$, is calculated as per the formula below, where a is the notch length and w is the sample width.

$$Y(\frac{a}{w}) = 1.93 - 3.07 \times (\frac{a}{w}) + 14.53 \times (\frac{a}{w})^2 - 25.11 \times (\frac{a}{w})^3 + 25.8 \times (\frac{a}{w})^4 \ldots\ldots\ldots\ldots (2)$$

K_{IC} was used to estimate the fracture energy (G_{Ic}), as per the following equation

$$G_{IC} = \frac{K_{IC}^{2}(1-v^{2})}{E} \,………........(3)$$

where E is the elastic modulus of the polymer, and v is the Poisson's ratio of epoxy (0.35). [34] For

each composition, at least five identical specimens were tested and the average results along with

the standard deviation have been reported.

High strain rate (~950-2500s^{-1}) mechanical testing of the samples under compression mode

was performed in a Split Hopkinson Pressure Bar (SHPB) (19.05 mm diameter, aluminum bars;

striker bar length = 3.05 m). For this purpose, polymer disks (5 mm x 1 mm) with uniform

surface were prepared in silicone molds before being subjected to loadings at high strain rates.

Annealed copper discs were used as pulse shapers to improve the dynamic equilibrium and also

dampen the high frequency components in the stress pulses thus reducing dispersive effects. The

results were compared with quasi-static compression testing (10 mm min^{-1}, strain rate = 0.02 s^{-1})), performed on samples with same dimensions, as employed during Split Hopkinson tests.

3. Results and Discussion

In this paper, we explore the potential of microporous MOF 5 towards toughening of a

cycloaliphatic epoxy resin. MOF 5 was prepared and used as filler for preparing epoxy

composites with improved mechanical properties.

3.1. Characterization of MOF 5

The powder diffraction pattern of MOF 5 is presented in Fig. 1. Rietveld analysis of our

diffraction pattern based on the structure reported in the literature (CCDC-277428) revealed the

existence of the cluster core as a regular Zn_4O tetrahedron, with a single central O atom bonded

to four Zn atoms that are further connected by 1,4 benzene dicarboxylic acid (BDC) linkers in paddle-wheel type fashion (Fig. 1).
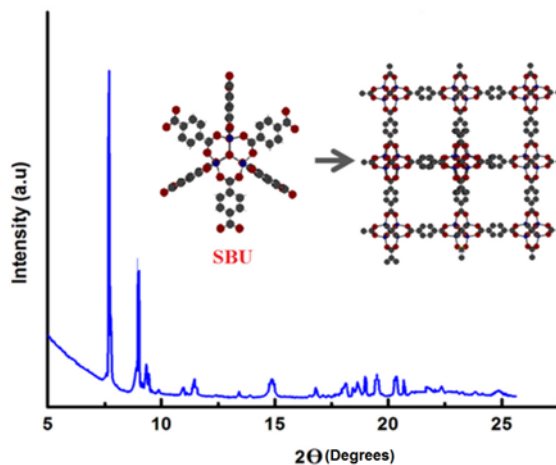

Fig. 1: PXRD of MOF 5. Inset shows the secondary building unit and crystal structure of the framework (Zn: blue; C: grey; H: white and O: red).

The nitrogen adsorption-desorption isotherm at 77 K is presented in Fig. 2. Open and filled symbols represent adsorption and desorption data respectively. The BET surface area was found to be 620 m^2 g^{-1}. SEM image of MOF 5 crystallites is also presented in the inset, which reveals the cube-like morphology of the obtained MOF 5 crystals.
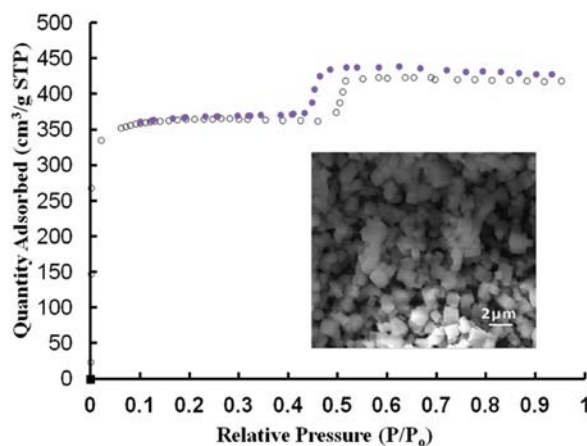

Fig. 2: N_2 adsorption and desorption isotherms for MOF 5. Inset shows the SEM image of MOF 5 crystallites. Adsorption: open symbols, desorption: filled symbols.

TG-DTG trace of MOF 5 is presented in Fig. 3. The initial mass loss of < 5% at ~300 °C can be attributed to the removal of DMF from the framework, which was followed by its pyrolytic decomposition at 410 °C leaving behind a char content of 42% at 600 °C.
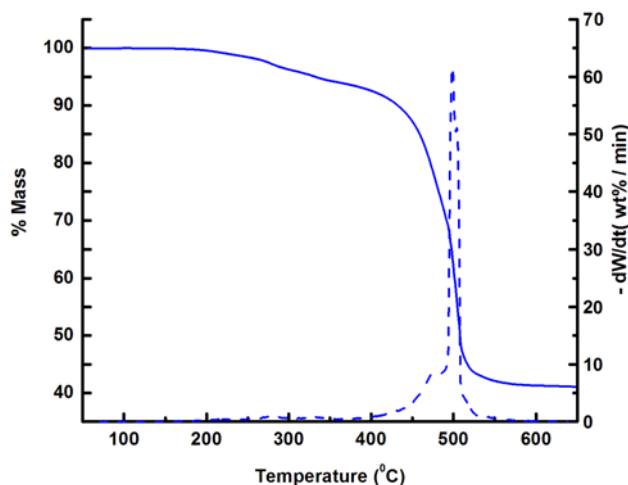

Fig. 3: TG -DTG traces of MOF 5.

The effect of MOF 5 on the physico-chemical properties of cycloaliphatic epoxy resin was studied under quasi-static and dynamic strain rate regimes.

3.2. MOF 5-Epoxy composites

Calorimetric traces associated with curing of neat epoxy and MOF 5 filled compositions are presented in Fig. 4(i). A single peak observed in all the traces characterizes the exothermic nature of epoxy curing. Incorporation of MOF 5 into the resin delayed the onset of the curing process appreciably with little change in curing enthalpy (ΔH_{cure}) as can be seen from Table 1. The onset cure temperature (T_{onset}) and peak cure temperature (T_{peak}) are also presented in Table 1. Interestingly, a significant increase in the glass transition temperature (T_g) (Fig. 4(ii)) was observed for all epoxy MOF 5 composites. Interestingly, epoxy-clay nanocomposites where the filler-matrix interface is weak have been reported to exhibit essentially no change in T_g and

damping.[35] In the present study, the observed increase in T_g value in epoxy-MOF 5 composites suggests a stronger interface between the epoxy and MOF 5 particles, which reduces the mobility of the chains around the high surface area microporous powder. Similar increase in T_g has been reported for CNT-epoxy composites, where CNT was surface functionalized to increase compatibility.[36]
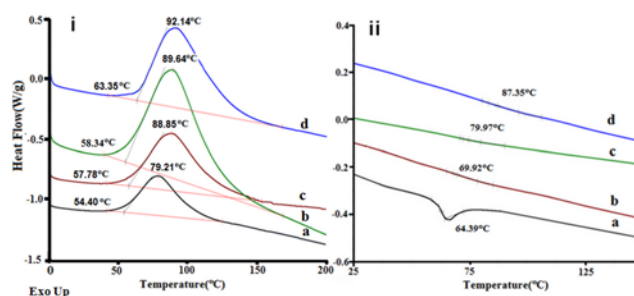

Fig. 4 (i) Curing profile of epoxy based compositions and (ii) DSC traces of cured samples a) Neat epoxy, b) EP1MOF, c) EP3MOF and d) EP7MOF

Table 1: Characteristic curing and thermal properties of epoxy and its composites

Sample	T_{onset} (°C)	T_{peak} (°C)	ΔH_{cure} (J/g)	T_g (°C)
Epoxy	56.4	79.2	280.0	64.4
EP1MOF	57.7	88.8	239.2	69.9
EP3MOF	58.3	89.6	495.2	79.9
EP5MOF	62.9	90.2	348.2	84.3
EP7MOF	63.3	92.1	324.1	87.3

The TG-DTG traces of epoxy and epoxy–MOF 5 composites are shown in Fig. 5. It can be seen that MOF 5 loadings in the concentration range under investigation did not affect the degradation profile of epoxy and all the compositions could be used till 250 °C. Double step decomposition was observed in all the samples where the pyrolytic decomposition of the main

chain occurred at ~350°C, reportedly leading to the formation of acetone, carbon dioxide, hydrogen cyanide and aliphatic hydrocarbons. [37]
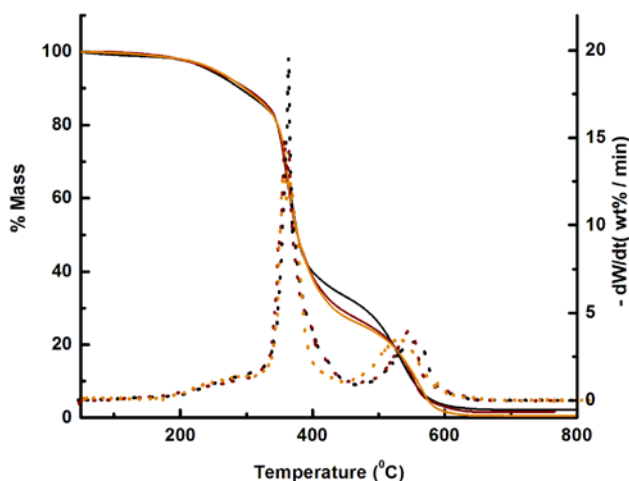

Fig. 5. TG-DTG traces of epoxy composites containing MOF 5. Solid lines indicative of TG and dashed lines represent DTG.

3.2. Quasi-static mechanical properties

Fig. 6 depicts the variation in tensile and compressive yield strength of epoxy–MOF 5 composites. It is observed that the characteristic mechanical properties of epoxy were substantially improved at MOF loadings ≤ 0.3 % w/w, which probably results from the homogeneous dispersion of the filler within the matrix.

In an earlier observation, introduction of mesoporous silica (SBA-15) resulted in overall toughening of epoxy, [38] which was attributed to intra-particle diffusion of epoxy within the mesopores of SBA-15 (pore dia ~ 5 nm). In MOF 5, the pore size is five times lower (~ 0.9 nm) [32, 39] and does not permit epoxy infiltration into the pores. It is speculated that the MOF 5 particles exist as elastic moieties which can elongate or compress depending on the type of load being applied. Moreover, the interactions between MOF 5 and the epoxy matrix are much

stronger because of the organic-inorganic hybrid nature of MOFs, which greatly influences the interfacial region. High specific surface area of MOF 5 leads to the creation of a large interfacial region in the composite, as the fraction of atoms localized at the surface is an order of magnitude than conventional fillers. The strong interface permits perfect load transfer from the matrix to the filler, which explains an observed increase in the mechanical properties. A significant increase in both strength and elongation was observed, which resulted in increased area under the stress-strain curve, implying enhancement in toughness.
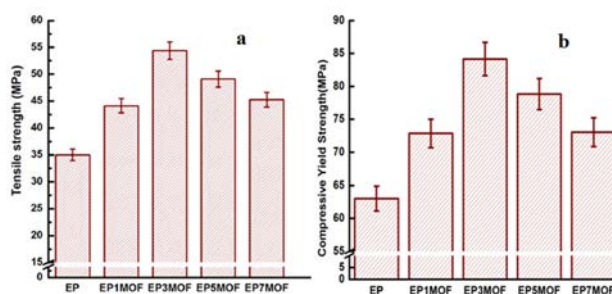

Fig.6. Variation of (a) tensile and (b) compressive yield strength with increasing concentration of MOF 5.

The effect of MOF 5 loading on the elastic modulus of epoxy (tensile mode) is depicted in Fig. 7. Significant stiffening of the base resin was observed as indicated by an increase in the tensile modulus, which can be attributed to the intrinsically high modulus of the crystalline MOF 5. [24] Uniaxial mechanical loading leads to stress concentration around the MOF 5 particles resulting in the formation of stress fields due to the difference in the Young's modulus. Previous theoretical studies have revealed that MOF 5 crystals are capable of exhibiting a high tensile modulus of 27.6 GPa along [100] as compared to 818 MPa for neat epoxy. However, increasing MOF 5 loading beyond 0.3% led to a decrease in the mechanical properties. Such an observation is not completely unexpected, in view of the exceptionally high surface area of microporous materials, which leads to their agglomeration, thereby restricting transfer of load. [36]
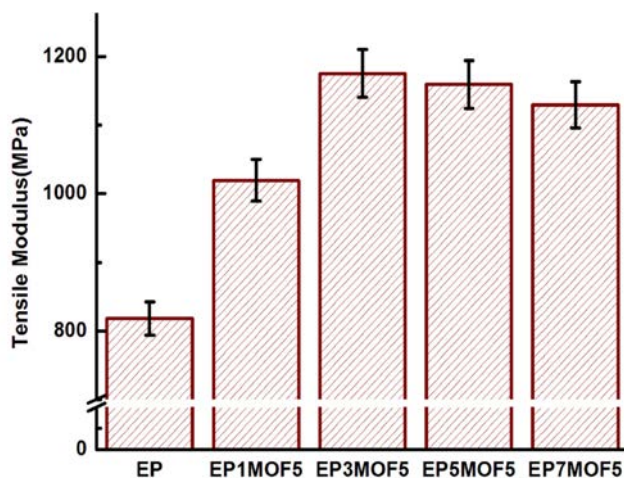
Fig. 7. Variation of elasticity with increasing concentration of MOF 5.

3.3. Impact properties

Izod impact strength was determined to quantify the amount of energy absorbed by the epoxy composites during fracture under low velocity conditions. The results of testing are presented in Fig. 8, which appear to follow a similar trend as observed during quasi-static tests. It can be seen that the impact strength improved with increasing MOF loading (till 0.3% w/w), and further loadings led to a decrease in the toughness, a feature attributable to the agglomeration of fillers which tend to act as weak links on being subjected to impact loadings.
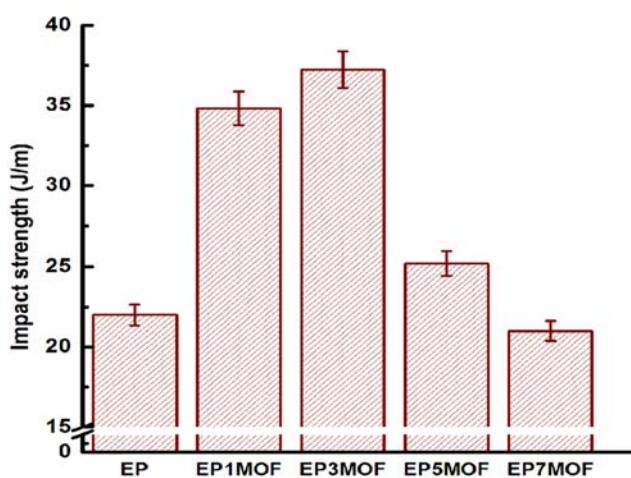

Fig.8: Variation of impact strength with increasing concentration of MOF 5.

3.4. Fracture properties

Mode I fracture toughness was determined by flexural three point bending tests. The results suggest that MOF 5 containing composites could be flexed to a higher extent, which in turn reflected in larger values of toughness, (Critical stress intensity factor, K_{IC}). The effect of MOF 5 on the K_{IC} and fracture energy (G_{IC}) is graphically shown in Fig. 9 a–b, respectively.

The K_{IC} of epoxy increased due to MOF 5 loading, from an initial value of 2.17 MPa $m^{1/2}$ for neat epoxy to 3 MPa $m^{1/2}$ for composites containing 0.3 % w/w of MOF 5 filler, corresponding to an increase of ~ 38%. The mean fracture energy also increased substantially on addition of MOF 5 and EP3MOF was found to possess ~236 % higher fracture energy as compared to the neat epoxy.
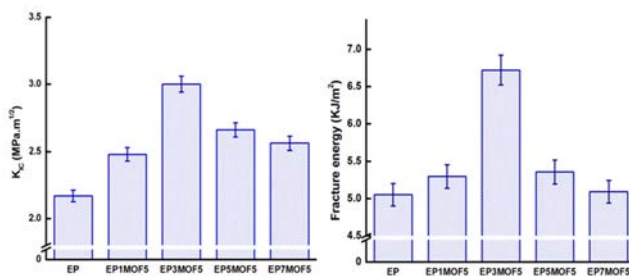

Fig. 9. Variation of a) K_{IC} and b) fracture energy with increasing concentration of MOF 5.

3.5. Dynamic Properties of composites

The variation of storage modulus and damping tan δ as a function of temperature and MOF 5 loading for neat epoxy and its composites are presented in Fig. 10. The glass transition temperatures (T_g) and the storage modulus (G') of the pristine cured epoxy resin was 66 °C and 2.73 GPa at 20° C respectively. In accordance with the quasi-static results, the composites exhibited higher storage modulus, especially at lower loadings of ≤ 0.3% w/w. A shift in the

temperature associated with the peak value of tan δ is in correspondence with the increase in T_g
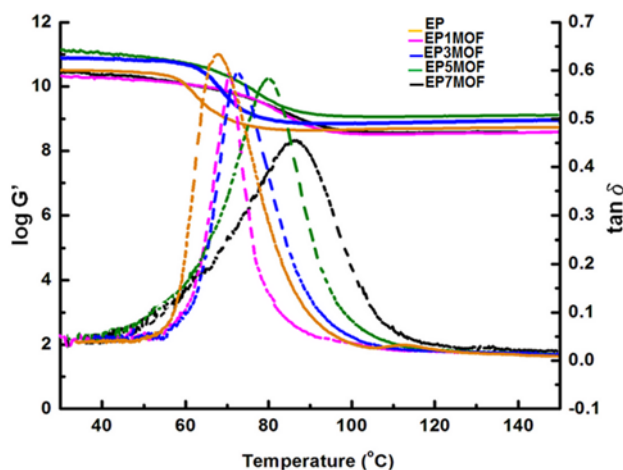
values of the composites.

Fig. 10. Storage modulus and damping tan δ traces for different compositions of epoxy-

composites. Solid lines indicate storage modulus and dashed lines present tan δ.

The damping behaviour of composites is also indicative of the extent of interfacial

adhesion of matrix with the fillers.[40] It can be seen from Fig. 10, that the magnitude of the tan δ

damping curve of the cured epoxy is significantly reduced upon compounding with MOF 5

particles, which is suggestive of the hindrance posed by the MOF particles towards the energy

dissipation process of epoxy.

3.5. Strain rate sensitivity

The strain rate sensitivity of a polymeric coating is of paramount importance, where there

is a possibility of the material to be used under blast loading conditions or projectile impacts.

Shock waves resulting from small scale bombings result in extremely high strain rates (10^3–10^4

15

s^{-1}) and the material behaviour of the composites under such conditions was evaluated experimentally using Split Hopkinson Pressure Bar (SHPB).

The true stress-strain compressive behaviour for a representative composite EP3MOF under quasi-static conditions and high strain rates (2393 s^{-1}) are presented in Fig. 11. It can be seen that increasing the strain rate led to substantial changes in characteristic mechanical properties, which was followed by the increase of the Property Enhancement Factor (PEF), defined as the ratio of the property at high strain rate loading to that under quasi-static conditions.[41] The slope of the stress-strain curve, indicative of the compressive modulus was found to increase substantially from 250 MPa under quasi-static conditions to 6.9 GPa at 2393s^{-1} corresponding to a PEF of 27.7. Also, at 10% true strain, the flow stress of the composite increased to ~110 MPa from 25 MPa under quasi-static conditions (PEF= 4.4). The material toughness was quantified by determining the area under the stress-strain trace (till 10 % strain), which increased from 1.2 MPa under quasi-static conditions to 13.1 MPa at high strain rates corresponding to a PEF of 10.9.

Theoretical studies on the mechanical response of another MOF, namely MIL-47 reveals that the paddle-wheel framework undergoes elastic deformation on being subjected to extreme compressive loadings of the order of ~340 MPa.[23] The present work generates experimental evidence that epoxy-MOF 5 composites can absorb significant amounts of energy even at high strain rates. Since the material toughness increases significantly upon increasing the strain rate, it can be concluded that these composites possess enormous potential as materials for blast mitigation.
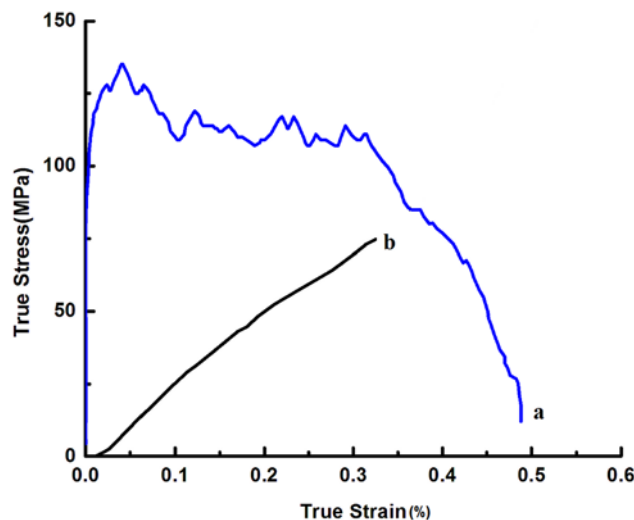
Fig. 11. Effect of strain rate on the compressive stress-strain curve of EP3MOF: a) 2393 s^{-1} and b) 0.02 s^{-1}

Numerical modeling was performed to simulate the behavior of epoxy retrofitting on the mechanical response of concrete on being subjected to blast loadings. The results are reported in the supplementary section. (Fig. S4-S5) under blast loadings, the target Laced Reinforced Concrete slab collapses completely resulting in the formation of fragments. Post-retrofitting with the epoxy-MOF 5 composite, the slab collapses but the fragments are arrested by the retrofit layer, thereby improving the level of safety. By improving mechanical properties of the polymer, its efficacy towards arresting fragments can be further increased, for a given layer thickness. Alternatively, for a given blast load, the thickness of the required retrofit layer can be brought down further, however these need to be substantiated by field trials, which are beyond the scope of the present study. However, the modeling results clearly point to the promising role of epoxy based polymeric retrofits in mitigating blast effects, their primary function being that of a fragment arrestor.

3.6. Toughening micromechanisms

To gain insight into the underlying mechanism behind the toughening of epoxy- MOF composites, fractographic analysis of the ruptured composite surfaces was performed. The SEM images of the surface of neat epoxy and EP3MOF are shown in Fig. 9. The smooth and featureless surface of neat epoxy is characteristic of its brittle failure (Fig. 9a,b). [42, 43] In comparison, the surface of fractured composite is rather rough. "Particle bridging" is the most commonly cited mechanism used to explicate the higher values of toughness in composites containing rigid particulates. It is envisaged that the MOF 5 particles tend to span the fracture surfaces formed as a result of crack propagation, thereby forming tractions, which in turn reduce the local stress at the propagating crack tip. In addition, substantial energy is expected to be consumed during the plastic deformation of the rigid MOF particles.

Another mechanism is that of toughening by "crack pinning", according to which, the role of rigid particles is to act as impenetrable objects that cause the crack front to bow out, thereby requiring larger amount of energy. Indirect evidence for the occurrence of this mechanism is the presence of 'tails' associated with the MOF 5 particles (Fig. 9c). In certain cases, the crack front is forced to change its path as it approaches the rigid phase, a phenomenon more commonly known as crack bowing, (Fig. 9d). This result in increased surface area and reduced nature of mode I character of the crack opening, which in turn leads to more energy consumption during crack propagation. In addition, evidence of "Microcracking" and "Crack path deflection" can also be seen in the SEM images. [7] It is conceivable that MOF 5 could promote the formation of a large number of subcritical microcracks and retard their collapse into critical cracks by coalescence. It is to be noted that quantification of each route to the total toughening of the composite is difficult, but nonetheless the SEM images appear to support the same. The ability of fillers to act as impact modifiers can only be exploited after its homogenous

dispersion within a host matrix; in this context, the hybrid nature of MOFs scores over carbon based solids and hence holds enormous potential as toughening agents.
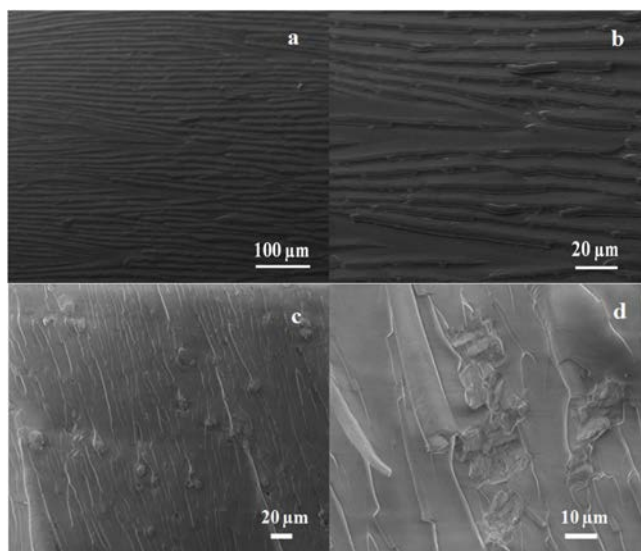

Fig. 12 : SEM images of fractured surface of neat epoxy (a-b) and EP3MOF (c-d) at different magnifications

Conclusions

Introduction of MOF 5 led to significant increase in the curing temperatures and the cured composites exhibited a higher glass transition temperature which was confirmed by dynamic mechanical analysis. Significant improvements in compressive and tensile mechanical properties were achieved at MOF 5 loadings of ≤ 0.3% w/w. A comparison of quasi-static compression testing with high strain rate studies using a Split Hopkinson pressure bar established the strain rate sensitivity of the epoxy MOF 5 composites. Fracture toughness and impact strength was found to increase by 236% and 68% respectively under optimal loadings of 0.3% w/w. The improvement in the mechanical property was attributed to the high surface area along

with the hybrid nature of the filler, which resulted in strong interfacial interaction between epoxy

resin and MOF 5 filler allowing perfect load transfer.

References

1. R. Bagheri and R. A. Pearson, *Polymer*, 1996, **37**, 4529-4538.
2. R. Bagheri and R. A. Pearson, *Polymer*, 2000, **41**, 269-276.
3. Y. L. Liang and R. A. Pearson, *Polymer*, 2010, **51**, 4880-4890.
4. Q.-H. Le, H.-C. Kuan, J.-B. Dai, I. Zaman, L. Luong and J. Ma, *Polymer*, 2010, **51**, 4867-4879.
5. S. Chaudhary, S. Parthasarathy, D. Kumar, C. Rajagopal and P. K. Roy, *J. App. Polym. Sci*, 2014, **131**.
6. P. Roy, N. Iqbal, D. Kumar and C. Rajagopal, *J. Polym. Res*, 2014, **21**, 1-9.
7. R. A. Pearson and A. F. Yee, *Polymer*, 1993, **34**, 3658-3670.
8. J. Choi, S. Lim, J. Kim and C.-R. Choe, *Polymer*, 1997, **38**, 4401-4406.
9. G. Cicala, A. Mamo, G. Recca and C. L. Restuccia, *Polym. Eng. Sci*, 2007, **47**, 2027-2033.
10. S. Chaudhary, S. Parthasarathy, D. Kumar, C. Rajagopal and P. K. Roy, *Polym. Compos*, 2014.
11. X. Xiao, S. Lu, B. Qi, C. Zeng, Z. Yuan and J. Yu, *RSC. Adv.*, 2014, **4**, 14928-14935.
12. Y. Li, R. Umer, A. Isakovic, Y. A. Samad, L. Zheng and K. Liao, *RSC. Adv.*, 2013, **3**, 8849-8856.
13. H. Zhang, L.-C. Tang, Z. Zhang, K. Friedrich and S. Sprenger, *Polymer*, 2008, **49**, 3816-3825.
14. J.-Y. Lee, M.-J. Shim and S.-W. Kim, *Polym. Eng. Sci*, 1999, **39**, 1993-1997.
15. J.-Y. Lee, M.-J. Shim and S.-W. Kim, *J. Mater. Sci*, 2001, **36**, 4405-4409.
16. S. Kang, S. I. Hong, C. R. Choe, M. Park, S. Rim and J. Kim, *Polymer*, 2001, **42**, 879-887.
17. S. T. Meek, J. A. Greathouse and M. D. Allendorf, *Adv. Mater*, 2011, **23**, 249-267.
18. S. L. James, *Chem.Soc. Rev*, 2003, **32**, 276-288.
19. J. L. C. Rowsell, E. C. Spencer, J. Eckert, J. A. K. Howard and O. M. Yaghi, *Science*, 2005, **309**, 1350-1354.
20. J. C. Tan and A. K. Cheetham, *Chem. Soc. Rev*, 2011, **40**, 1059-1080.

21.   A. Kuc, A. Enyashin and G. Seifert, *The J. Phy. Chem. B*, 2007, **111**, 8179-8186.
22.   A. U. Ortiz, A. Boutin, A. H. Fuchs and F.-X. Coudert, *Phy. Rev. Lett*, 2012, **109**, 195502.
23.   P. G. Yot, Q. Ma, J. Haines, Q. Yang, A. Ghoufi, T. Devic, C. Serre, V. Dmitriev, G. Ferey, C. Zhong and G. Maurin, *Chem. Sci,* 2012, **3**, 1100-1104.
24.   D. F. Bahr, J. A. Reid, W. M. Mook, C. A. Bauer, R. Stumpf, A. J. Skulan, N. R. Moody, B. A. Simmons, M. M. Shindel and M. D. Allendorf, *Phy. Rev. B*, 2007, **76**, 184106.
25.   Q. Wei, H. W. Xu, X. H. Yu, T. Shimada, M. S. Rearick, D. D. Hickmott, Y. S. Zhao and S. N. Luo, *J. App. Phy*, 2011, **110**, 056102-056103.
26.   A. Kathuria, M. G. Abiad and R. Auras, *Polymer*, 2013, **54**, 6979-6986.
27.   D. Elangovan, U. Nidoni, I. E. Yuzay, S. E. M. Selke and R. Auras, *Ind. Eng. Chem. Res*, 2011, **50**, 11136-11142.
28.   D. Elangovan, I. E. Yuzay, S. E. M. Selke and R. Auras, *Polym. Inter*, 2012, **61**, 30-37.
29.   C. Zilg, R. Thomann, J. Finter and R. Mülhaupt, *Macromol.Mater. Eng*, 2000, **280-281**, 41-46.
30.   X. Ji, J. E. Hampsey, Q. Hu, J. He, Z. Yang and Y. Lu, *Chem. Mater*, 2003, **15**, 3656-3662.
31.   Manju, P. Kumar Roy, A. Ramanan and C. Rajagopal, *Mater. Lett*, 2013, **106**, 390-392.
32.   Manju, P. K. Roy, A. Ramanan and C. Rajagopal, *RSC. Adv*, 2014, **10.1039/c4ra00894d**.
33.   J. F. Knott, *Fundamentals of Fracture Mechanics*, Butterworths, London,, 1976.
34.   A. J. Kinloch, *Adhesion and adhesives: science and technology.*, Chapman & Hall, London, 1987.
35.   E. Kaya, M. Tanoğlu and S. Okur, *J. Appl. Polym. Sci.*, 2008, **109**, 834-840.
36.   Y. X. Zhou, P. X. Wu, Z. Y. Cheng, J. Ingram and S. Jeelani, *Express. Polym. Lett*, 2008, **2**, 40-48.
37.   J. Vogt, *Thermochim. Acta*, 1985, **85**, 411-414.
38.   P. K. Roy, A. V. Ullas, S. Chaudhary, V. Mangla, P. Sharma, D. Kumar and C. Rajagopal, *Iran. Polym. J*, 2013, 1-11.
39.   H. Kim, S. Das, M. G. Kim, D. N. Dybtsev, Y. Kim and K. Kim, *Inorg. Chem*, 2011, **50**, 3691-3696.
40.   J. Ma, M.-S. Mo, X.-S. Du, P. Rosso, K. Friedrich and H.-C. Kuan, *Polymer*, 2008, **49**, 3510-3523.
41.   G. Ravikumar, J. R. Pothnis, M. Joshi, K. Akella, S. Kumar and N. K. Naik, *Mater. Des.*, 2013, **44**, 246-255.
42.   J. G. Williams, *Compos. Sci. Technol*, 2010, **70**, 885-891.
43.   R. Voo, M. Mariatti and L. C. Sim, *Compos. Part B: Eng*, 2012, **43**, 3037-3043.

Graphical Abstract
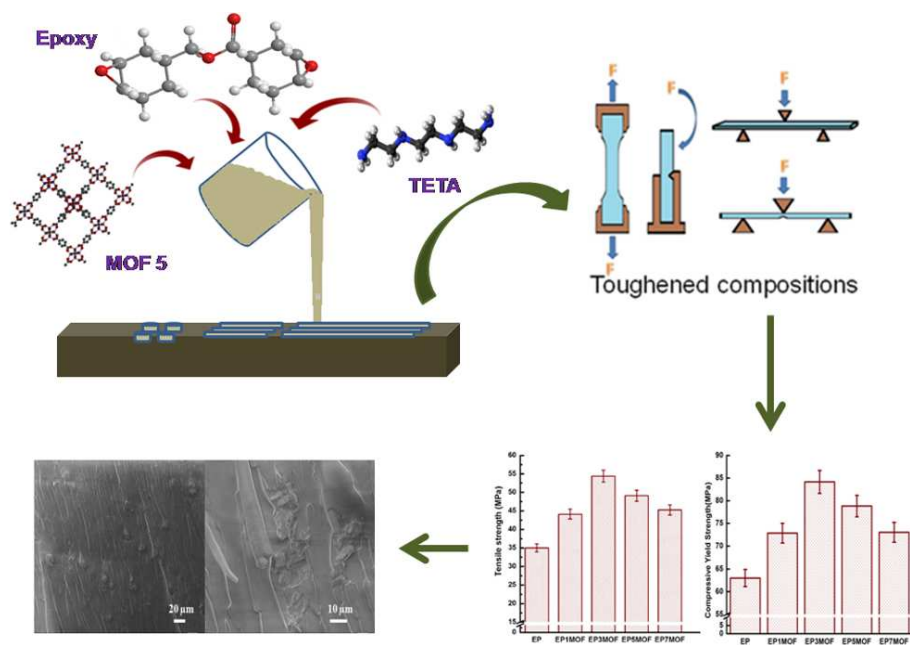
The potential of metal organic frameworks (MOF 5) towards toughening of brittle

cycloaliphatic epoxy thermosetting resin has been demonstrated.